Report

Current Biology

# Pattern differentiation and tuning shift in human sensory cortex underlie long-term threat memory

## Highlights

- Threat conditioning produces long-term affective and perceptual memory
- Associative plasticity emerges in human primary olfactory (piriform) cortex
- The piriform cortex exhibits long-term pattern differentiation and tuning shift
- These sensory cortical underpinnings of threat memory are hyperactive in anxiety

## Authors

Yuqi You, Lucas R. Novak, Kevin J. Clancy, Wen Li

## Correspondence

youlilly@gmail.com (Y.Y.), wenli@psy.fsu.edu (W.L.)

## In brief

Rapidly accruing evidence questions amygdala's dominance in (human) threat processing. Favoring a distributed threat circuitry, You et al. identify long-term threat memory in human sensory (olfactory) cortex (but not amygdala or orbitofrontal cortex). Notably, this sensory cortical memory system hyperfunctions in anxiety.

You et al., 2022, Current Biology *32*, 2067–2075
May 9, 2022 
https://doi.org/10.1016/j.cub.2022.02.076

CellPress

Current Biology

CellPress

Report

# Pattern differentiation and tuning shift in human sensory cortex underlie long-term threat memory

Yuqi You,[1,*] Lucas R. Novak,[1] Kevin J. Clancy,[1] and Wen Li[1,2,3,*]
[1]Department of Psychology, Florida State University, 1107 W. Call St., Tallahassee, FL 32306, USA
[2]Twitter: @wenlicanlab
[3]Lead contact
*Correspondence: youlilly@gmail.com (Y.Y.), wenli@psy.fsu.edu (W.L.)
https://doi.org/10.1016/j.cub.2022.02.076

## SUMMARY

The amygdala-prefrontal-cortex circuit has long occupied the center of the threat system,[1] but new evidence has rapidly amassed to implicate threat processing outside this canonical circuit.[2–4] Through nonhuman research, the sensory cortex has emerged as a critical substrate for long-term threat memory,[5–9] underpinned by sensory cortical pattern separation/completion[10,11] and tuning shift.[12,13] In humans, research has begun to associate the human sensory cortex with long-term threat memory,[14,15] but the lack of mechanistic insights obscures a direct linkage. Toward that end, we assessed human olfactory threat conditioning and long-term (9 days) threat memory, combining affective appraisal, olfactory psychophysics, and functional magnetic resonance imaging (fMRI) over a linear odor-morphing continuum (five levels of binary mixtures of the conditioned stimuli/CS+ and CS− odors). Affective ratings and olfactory perceptual discrimination confirmed (explicit) affective and perceptual learning and memory via conditioning. fMRI representational similarity analysis (RSA) and voxel-based tuning analysis further revealed associative plasticity in the human olfactory (piriform) cortex, including immediate and lasting pattern differentiation between CS and neighboring non-CS and a late onset, lasting tuning shift toward the CS. The two plastic processes were especially salient and lasting in anxious individuals, among whom they were further correlated. These findings thus support an evolutionarily conserved sensory cortical system of long-term threat representation, which can underpin threat perception and memory. Importantly, hyperfunctioning of this sensory mnemonic system of threat in anxiety further implicates a hitherto underappreciated sensory mechanism of anxiety.

## RESULTS

### Behavioral effects

As in previous nonhuman[12,16,17] and human[18] research, we employed a linear morphing continuum of odor mixtures, with the two extreme odor mixtures (i.e., threat CS [CSt] and safety CS [CSs]) differentially paired with bimodal unconditioned stimuli (UCS) (i.e., aversive or neutral sounds and images; Figures 1A–1C). We examined threat learning and long-term (9 days) threat memory based on affective appraisal and perceptual discrimination (in an odor discrimination task [ODT]) of the CS.

#### *Affective appraisal*

Pre-experiment odor valence ratings (on a visual analog scale [VAS] of 0–100) indicated neutral affective values for the five odors, conforming to a flat neutral baseline over the odor continuum ($p = 0.416$; mean [SD] = 50.6 [19.7]). Risk ratings of the odors (i.e., the likelihood of aversive UCS following a given odor) were acquired postconditioning on day 1 and day 9. Consistent with our hypothesis (Figure 2A), an ANOVA of odor (five odors) and time (day 1/day 9) demonstrated a strong ascending linear trend over the odor continuum ($F_{1,30} = 6.99$, $p = 0.013$; Figure 2C). There was no odor-by-time interaction ($p = 0.908$), suggesting equivalent trends for day 1 and day 9. Akin to the linear trend, CSt and CSs had maximal and minimal risk ratings, respectively (CSt versus CSs: $t_{31} = 3.02$, $p = 0.005$), deviating from the neutral level (50%) in opposite directions (CSt: $t_{31} = 2.67$, $p = 0.012$; CSs: $t_{31} = -2.40$, $p = 0.023$). Ratings for the three nonconditioned stimuli (nCS) odors remained neutral on both days (49.3%–51.3%; all p values > 0.581) and comparable with each other ($F_{1,31} = 0.14$, $p = 0.708$) but differed from CSt and CSs in opposing directions (neighboring CSt [nCSt] versus CSt: $t_{31} = -2.41$, $p = 0.022$; nCSs versus CSs: $t_{31} = 1.92$, $p = 0.032$ one-tailed). These results thus confirmed that our differential conditioning produced a threat and a safety CS that persisted till day 9, with limited generalization to the non-CS.

#### *Perceptual discrimination*

Akin to the linear odor-morphing continuum, baseline ODT performance conformed to a strong linear trend of increasing endorsement of the dominant odor of the CSt (i.e., "CSt" rate), $F_{1,31} = 79.62$, $p < 0.0001$ (Figures 2B and 2D). We hypothesized that differential conditioning would expand perceptual distances (i.e., enhance perceptual discrimination) between the CS and their neighboring nCS. Across the odor continuum, this expansion would manifest as a cubic pattern of differential "CSt" rates (postconditioning minus preconditioning), anchored by respective

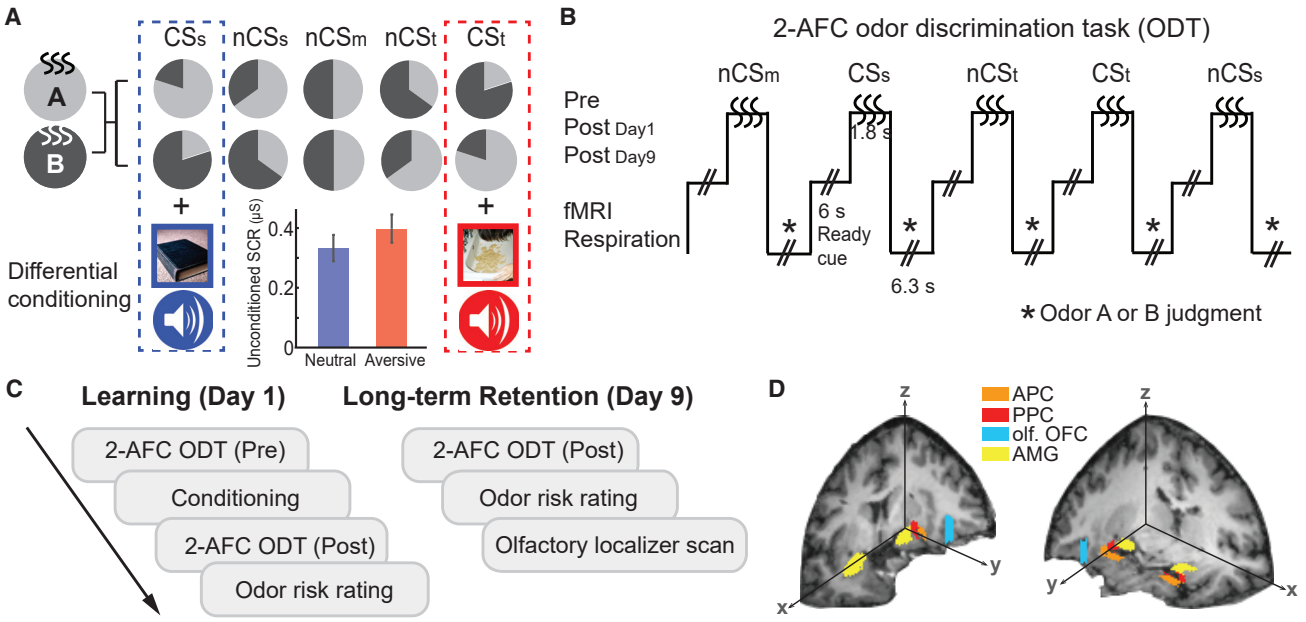


**Figure 1. Odor stimuli and experimental design**

(A) Stimuli consisted of a continuum of five parametrically morphed binary odor mixtures of neutral odors (acetophenone and eugenol labeled as odor A and odor B). The extreme mixtures (20% A/80% B and 80% A/20% B; to rule out confounds related to pure or mixture odorants, all stimuli consisted of binary mixtures) were differentially conditioned as CSt (threat) or CSs (safety) via paired presentation with aversive or neutral unconditioned stimuli (UCS: bimodal aversive or neutral pictures and sounds). SCR evoked by the aversive (versus neutral) UCS confirmed their effectiveness (aversive versus neutral: $t = 2.88$; $p = 0.007$). Assignment of CSt/CSs was counterbalanced across participants. The three intermediate mixtures (35% A/65% B, 50% A/50% B, and 65%A/35% B) were nonconditioned stimuli (nCS), representing the odor neighboring CSt (nCSt), the midpoint mixture (nCSm), and the odor neighboring CSs (nCSs). Error bars represent standard error.

(B) Two-alternative-forced-choice (2-AFC) odor discrimination task (ODT) accompanied by fMRI and respiration acquisition. Each trial presented an odor mixture pseudorandomly for 1.8 s, to which participants made judgments of "odor A" or "odor B" with button pressing.

(C) Experiment schedule. Day 1 consisted of preconditioning 2-AFC ODT, conditioning, postconditioning 2-AFC ODT, and odor risk rating. Day 9 consisted of postconditioning 2-AFC ODT, odor risk rating, and an olfactory localizer scan.

(D) Regions of interest (ROIs). Anatomical masks of the primary olfactory cortex (anterior piriform cortex [APC] and posterior piriform cortex [PPC]), the olfactory orbitofrontal cortex ($OFC_{olf}$), and the amygdala (AMG) are displayed on 3D T1 sections of one participant. These ROIs were further functionally constrained by the olfactory localizer.

See also Figure S1.

increase and decrease (from pre- to post-conditioning) in "CSt" rate for the neighboring odors of CSt and CSs—nCSt and nCSs (Figure 2B [inset]). Indeed, an ANOVA of odor (five odors) and time (day 1/day 9) on differential "CSt" rates confirmed this cubic trend ($F_{1,31} = 3.16$, $p = 0.043$ one-tailed; Figure 2D [inset]). Like risk ratings, there was no odor-by-time interaction ($p = 0.405$), suggesting equivalent changes for day 1 and day 9. The expansion between the CS and neighboring nCS was further ascertained in a follow-up ANOVA (odor: nCSt/nCSs by time: day 1/day 9 on differential "CSt" rates). We observed an odor effect ($F_{1,31} = 5.19$, $p = 0.030$) and, specifically, a negative differential "CSt" rate for the nCSt odor (i.e., less CSt endorsement and greater perceptual distance from CSt postconditioning) and a positive differential "CSt" rate for the nCSs odor (i.e., more CSt endorsement and greater perceptual distance from CSs postconditioning; Figure 2D [inset]). Again, this ANOVA showed no odor-by-time interaction ($p = 0.427$), suggesting equivalent effects for both days. Therefore, differential conditioning warped odor quality space, particularly expanding perceptual distances between the CS and neighboring nCS. Overall, results in affective appraisal and perceptual discrimination converged to confirm threat learning and long-term memory in the participants.

## Neural effects

Nonhuman research has evinced plasticity associated with conditioning in the sensory cortex that arises immediately and lasts for days to weeks,[19–21] serving a critical role in the formation[5,22–24] and storage of long-term memory of conditioning.[22,25–28] In humans, threat conditioning also induces immediate sensory cortical plasticity.[18,29–34] Recently, a link between human sensory cortex and long-term memory of conditioning has begun to emerge, indicated by enduring (15-day long) plasticity in human visual cortex (i.e., enhanced V1/V2 response to CS)[14] and impairment in delayed (24 h) conditioned response following inhibitory stimulation of human somatosensory cortex.[15]

Nonhuman research has revealed pattern separation/completion in the sensory (particularly, olfactory) cortex to underpin memory of conditioning.[10,11] The olfactory primary (piriform) cortex is considered an associative, content-addressable memory system and thus ideally positioned to store long-term memory of conditioning.[8,35,36] Nonhuman research has further implicated "associative representational plasticity" as a mechanism of long-term memory and sharpened perception of the CS.[12] This plasticity is characterized by sensory cortical tuning shift, i.e., sensory cortical neurons initially tuned to non-CS become

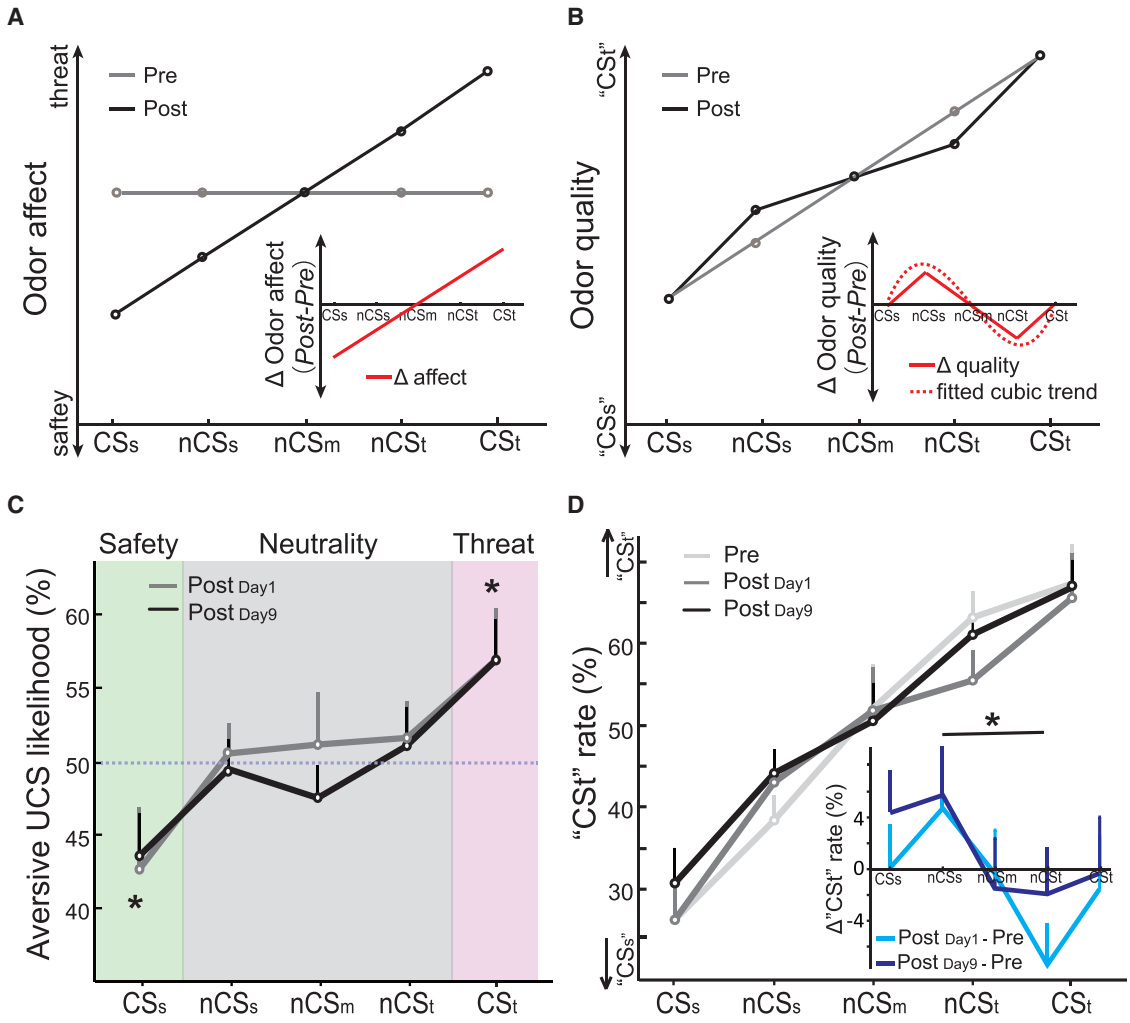


**Figure 2. Behavioral effects of olfactory conditioning**

(A) Hypothetical affective space over the odor continuum: the initial neutral baseline (gray line) would change to an ascending safety-to-threat line (black line) after acquiring affect (safety/threat) through differential conditioning. Inset shows changes (Δ; post–pre) in odor affect over the continuum via conditioning, which confirms to a linear trend.

(B) Hypothetical perceptual (quality) space over the odor continuum: the initial ascending trend (gray line: tracking the linear increase in the proportion of CSt) would be warped after conditioning due to expanded distances (i.e., enhanced perceptual discrimination) between the CS (CSt/CSs) and neighboring nCS (nCSt/nCSs) (black line). Inset illustrates the changes (Δ; post−pre) in perceived odor quality (solid line), which can be fitted by a cubic trend, anchored by respective increase and decrease in "CSt" rate for nCSt and nCSs (dotted line).

(C) Empirical risk ratings (likelihood of aversive UCS) on both days conformed to the predicted profile of differential conditioning: below-chance risk for CSs and above-chance risk for CSt. Risks for the three intermediate mixtures remained chance level (50%; indicated by the dotted line).

(D) Empirical 2-AFC ODT performance ("CSt" responses rate) over the CSs-to-CSt continuum conformed to a linear trend before conditioning, which was warped after conditioning. Inset illustrates differential (Δ) "CSt" rates (post−pre) over the odor continuum on day 1 and day 9, which largely conformed to the hypothesized cubic trend. Specifically, perceptual distances between the CS and neighboring nCS increased after conditioning, with the nCSt odor less endorsed as "CSt" and the nCSs odor more endorsed as "CSt" (i.e., less as "CSs"). Error bars represent SE. (individually adjusted SEM). *$p < 0.05$.

preferentially tuned to the CS.[9,13,19,20] Critically, this plasticity would consolidate over time and last for a long time, thereby underpinning stable sensory representation and long-term memory of CS.[7,12,13,37]

We thus interrogated whether threat conditioning would induce long-term pattern differentiation and tuning shift in the human olfactory cortex (anterior and posterior piriform cortices [APC/PPC]) using functional magnetic resonance imaging (fMRI) representational similarity analysis (RSA)[29] and voxel-based tuning analysis,[38,39] respectively. To compare the sensory cortex with the canonical amygdala-prefrontal-cortex circuit, supplemental analyses further explored these processes in the amygdala and orbitofrontal cortex (OFC; Figure 1D). Importantly, given that threat learning and memory represents an eminent model of anxiety disorders,[4,40,41] we examined individual differences in sensory cortical associative plasticity as a function of anxiety, thereby identifying a sensory cortical underpinning of anxiety.

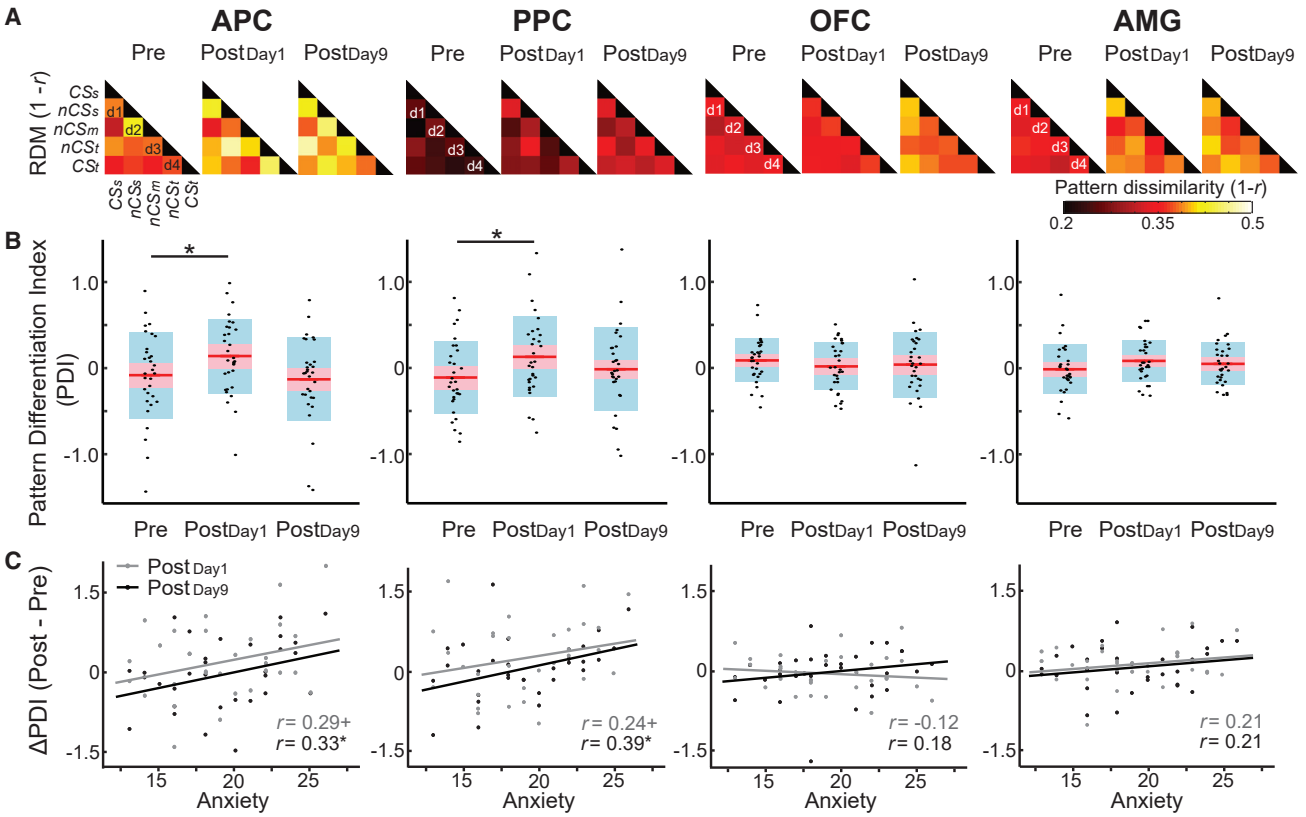


**Figure 3. Olfactory cortical pattern differentiation between CS and neighboring nCS odors**

(A) Group-average representational dissimilarity matrices (RDMs) for APC, PPC, OFColf, and amygdala (AMG) at each phase. Each cell of the matrix indicates pattern dissimilarity ($1 - r$), reflecting pattern differentiation, for a given odor pair. Cells right off the diagonal indicate pattern differentiation between neighboring odors: CSs and nCSs (d1), nCSs and nCSm (d2), nCSm and nCSt (d3), and nCSt and CSt (d4). Based on that, we derived a pattern differentiation index (PDI) for the CS and the neighboring nCS [PDI = (d1 + d4) − (d2 + d3)].

(B) PDI for each ROI at preconditioning, day 1, and day 9 postconditioning. Both APC and PPC (but neither amygdala nor OFC) demonstrated increased PDI from preconditioning to postconditioning on day 1, but not on day 9. Center red line, group mean; red and blue boxes, 95% confidence interval and mean ± 1 SD, respectively.

(C) Correlations between conditioning-induced PDI changes and anxiety. PDI changes on day 9 (versus pre) in the APC and PPC correlated positively with anxiety, indicating persistent pattern differentiation in anxious individuals. *p < 0.05; +p < 0.1.

See also Figure S2.

## Plasticity in the olfactory cortex

### *Pattern differentiation*

Immediate pattern differentiation for CS has been observed in the human piriform cortex,[29] which, we hypothesized, would persist to support long-term threat memory. RSA was applied to extract a pattern differentiation index (PDI), reflecting pattern dissimilarity (i.e., pattern differentiation) between the CS and its neighboring nCS (Figure 3). ANOVAs of region of interest (ROI) (APC/PPC) and time (day 9/day 1) on the differential PDI (postconditioning minus preconditioning) showed a main effect of time, $F_{1,30}$ = 4.30, p = 0.047. This time effect reflected significant PDI increase in the piriform (APC/PPC) cortex ($t_{30}$ = 1.91, p = 0.033 one-tailed) on day 1, in contrast to no PDI increase on day 9 (all p values > 0.366). Interestingly, PDI increase in the piriform cortex on day 9 correlated positively with anxiety ($r$ = 0.40, p = 0.025, FDR p < 0.05; Figure 3C), indicating that olfactory cortical pattern differentiation persisted among anxious individuals. There was no effect of ROI (p = 0.296) or interaction (p = 0.271): as illustrated in Figures 3A and 3B, APC and PPC showed similar, significant PDI increase on day 1 and similar significant correlation between PDI increase on day 9 and anxiety. Finally, these results were confirmed by nonparametric tests and leave-one-out cross-validation (supplemental information; Table S1).

### *Tuning shift*

We then examined tuning shift toward CS in the piriform cortex, i.e., whether voxels initially responded maximally to neighboring odors of the CS (i.e., nCSt and nCSs) became maximally responsive to the CS after conditioning.[12,42] Before conditioning, tuning was evenly distributed across the morphing continuum in the piriform cortex (and the supplemental regions—amygdala and OFC); i.e., equivalent % of voxels tuned to the five odors (all $F$ values < 1.88; p values > 0.125). An ANOVA of ROI (APC/PPC) and time (day 9/day 1) on tuning shift index (TSI; % of nCS voxels toward the neighboring CS versus the neighboring nCS) revealed a significant ROI-by-time interaction ($F_{1,30}$ = 6.99, p = 0.013) and no main effect of ROI (p = 0.379) or time (p = 0.612). Specifically, the interaction reflected significant TSI in the PPC on day 9 ($t_{30}$ = 3.00, p = 0.005; FDR

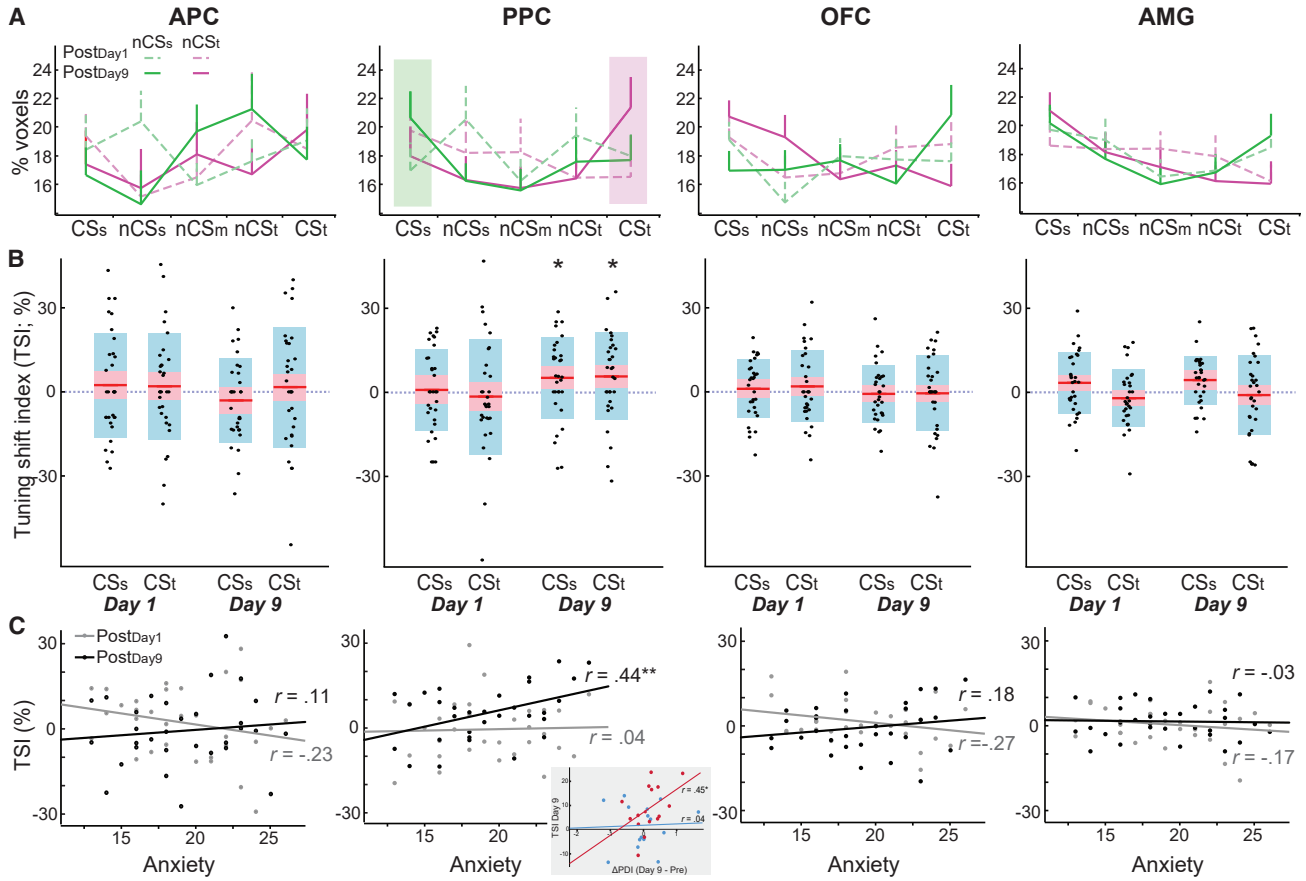


**Figure 4. Olfactory cortical tuning shift toward the CS**

(A) Day 1 (dashed lines) and day 9 (solid lines) postconditioning tuning profiles of nCSs (green) and nCSt (pink) voxels (i.e., respectively, tuned to nCSs and nCSt at the baseline). In PPC on day 9, the nCS voxels exhibited a strong tuning preference for their respective CS: highest % of nCSs voxels tuned to CSs (shaded in green) and highest % of nCSt voxels tuned CSt (shaded in pink).

(B) Tuning shift index (TSI; % of nCS voxels toward respective CS versus the middle nCS) on day 1 and day 9 postconditioning. On day 9, PPC showed significant TSI for both nCSs and nCSt voxels toward their respective CS (CSs and CSt, respectively). The dotted line indicates zero tuning shift (TSI = 0). Center red line, group mean; red and blue boxes, 95% confidence interval and mean ± 1 SD, respectively.

(C) Correlations between anxiety and tuning shift toward CS (collapsed across nCSs and nCSt). Day 9 TSI in the PPC correlated positively with anxiety, indicating amplified tuning shift in anxious individuals. The inset: in anxious (red dots), but not in nonanxious (blue dots), participants, day 9 PPC TSI correlated with day 9 PPC PDI increase (more details in supplemental information; Figure S2). *p < 0.05; **p < 0.01.

See also Figure S2.

p < 0.05) but not on day 1 (p = 0.802) or in the APC on either day (all p values >0.269; Figures 4A and 4B). Interestingly, PPC TSI on day 9 positively correlated with anxiety, suggesting that anxiety potentiated this delayed PPC tuning shift ($r$ = 0.44, p = 0.014; FDR p = 0.056; Figure 4C). Finally, these results were confirmed by nonparametric tests and leave-one-out cross-validation (supplemental information; Table S2).

### *Association between pattern differentiation and tuning shift via conditioning*

Results above showed that pattern differentiation and tuning shift were both present on day 9 among anxious participants. We thus explored the inherent association between these plastic processes and found that PDI change and TSI in the PPC on day 9 were correlated in the high-anxiety group (based on median split; $r$ = 0.45, p = 0.039 one-tailed; Figures 4C [inset] and S2). By contrast, there was no correlation ($r$ = 0.04, ns) in the low-anxiety group. These results confirm the shared origin of these plastic processes in threat conditioning and anxiety.

### Plasticity in the amygdala and OFC

We then explored pattern differentiation and tuning shift in the amygdala and OFC. As for pattern differentiation, the amygdala showed a marginal increase in PDI on day 1 ($t_{30}$ = 1.48, p = 0.075 one-tailed) but not on day 9 (p = 0.413; Figures 3A and 3B). The PDI scores on neither day were correlated with anxiety (all p values > 0.252; Figure 3C). The OFC showed no PDI increase nor correlations of PDI increase with anxiety (all p values > 0.292). As for tuning shift, TSI in the amygdala and OFC showed no significant tuning shift on either day (all p values > 0.169) nor correlation with anxiety (all p values > 0.144; Figure 4). Therefore, in contrast to the olfactory cortex, the canonical amygdala-OFC

circuit failed to exhibit clear pattern differentiation or tuning shift following conditioning.

## DISCUSSION

We demonstrated affective and perceptual learning and long-term memory, accompanied by immediate and lasting pattern differentiation as well as late-onset, lasting tuning shift in the human olfactory cortex, especially among anxious individuals. These findings highlight the role of the human sensory cortex in threat memory and advance the extant (human and non-human) literature of anxiety modulation of the sensory cortical system of threat memory. Together, they illuminate hitherto underexplored human sensory mechanisms of threat processing and their contribution to the pathophysiology of anxiety.

Differential conditioning is known to promote divergent conditioned responses to (threat and safety) CS, minimizing conditioning generalization and facilitating CS discrimination (especially from similar stimuli).[17,29,43,44] Our risk ratings over a parametrically morphed odor continuum confirmed differential affective learning and memory for CSt and CSs and minimal generalization to the nCS. Our ODT further demonstrated perceptual (discrimination) learning and memory for CS (versus neighboring nCS). Together, differential conditioning warped both affective and perceptual spaces over the continuum, expanding the distance between the CS and their neighboring nCS and compressing the distance among the nCS. Such paralleled reorganization of affective and perceptual spaces reiterates that acquisition and generalization/specification of threat response tracks the perceptual distance between the CS and nCS.[45–47]

Neurally, the olfactory (APC and PPC) cortex exhibited immediate and lasting pattern differentiation between the CS and neighboring nCS, especially in anxious individuals. This pattern differentiation resembles conditioning-induced pattern separation in nonhuman sensory cortex, underpinning CS memory representation[10,11] as a "perceptual-mnemonic" mechanism.[48] It is yet unclear whether this process directly relates to hippocampal pattern separation characterized by sparse orthogonalized representation.[49,50] The human PPC is a critical site for olfactory sensory representation and underpins odor object encoding.[51,52] The immediate effect in PPC replicates our previous finding, reflecting adapted sensory representation of CS.[29] The lasting effect in PPC suggests that this plasticity would persist to support enduring sensory cortical representation of CS as part of the long-term memory of acquired threat/safety. The APC exhibited a comparable effect, replicating decorrelation of APC responses to CS and similar nCS in rodents.[10,17] Given human APC's role in olfactory attention and arousal,[52] this APC pattern differentiation could reflect heightened sensory vigilance to CS.

The other mnemonic mechanism—tuning shift that underpins associative representational plasticity—is also confirmed here in humans, particularly in the PPC. Interestingly, this plastic process was observed on day 9 only. This temporal profile accords with nonhuman findings: sensory cortical tuning shift is relatively weak in magnitude and specificity immediately after conditioning but becomes stronger over time (days and weeks).[19] It also coincides with our recent finding of delayed (day 16, but not immediate) plasticity in human primary visual cortex (V1/V2).[14] Therefore, this tuning shift, particularly in the PPC that is critical for olfactory sensory representation, underscores time-dependent associative representational plasticity in human olfactory cortex to support enduring CS representation as part of long-term memory of acquired threat/safety.[7,19]

In comparison, the amygdala and OFC exhibited no clear evidence of pattern differentiation or tuning shift by conditioning. The null findings here highlight the human sensory cortex (outside the canonical threat circuit) as an independent neural substrate for threat memory. That said, we analyzed these processes expressly along a physical dimension (i.e., odor-morphing continuum) to elucidate neural representation of CS sensory input, which does not rule out amygdala/OFC associative plasticity in other, abstract dimensions (e.g., valence or value). In fact, previous research comparing (immediate, appetitive) conditioning effects in the rodent piriform cortex and OFC has revealed sensory-based plasticity in the former and value/rule-based plasticity in the latter (e.g., [53]). Similarly, human research of (both appetitive and aversive) conditioning has underscored value-based (versus sensory-based) pattern differentiation in the OFC and amygdala.[29,54,55] In sum, the contrast here highlights a sensory-bound representation system of threat memory ("S-memory")[56,57] in the sensory cortex.

Finally, leveraging self-report from human participants, we demonstrated that anxiety amplified these threat mnemonic processes in the sensory cortex. Similar to our recent finding in the visual cortex,[14] anxiety particularly heightened piriform plasticity on day 9. This anxiety effect helps to reconcile the seeming temporal dissociation between *group-level* (average) effects of pattern differentiation (present on day 1) and tuning shift (present on day 9), that is, in anxious individuals, the two forms of plasticity were both present on day 9 and, moreover, correlated with each other, highlighting their shared origin in threat conditioning and anxiety. We caution that our sample could be small for a study of individual differences, warranting replication through future large-scale studies. Nonetheless, findings of sensory-based long-term threat memory in anxiety lend direct credence to anxiety theories centered on hyperactive sensory memory of threat.[56,57] They also confer mechanistic insights into intrusive memories (a hallmark symptom) in post-traumatic stress disorder (PTSD) laden with vivid sensory fragments of trauma and readily triggered by simple sensory cues.[58–60]

To conclude, lasting pattern differentiation and tuning shift in the human PPC, paralleling long-term threat memory, provides mechanistic evidence for the human sensory cortex as a key component of the threat circuitry. This long-term threat representation may serve to underpin threat processing in the sensory cortex, even in the initial feedforward sweep.[61–63] Importantly, that this sensory cortical mnemonic system of threat is hyperfunctioning in anxiety adds to the growing support for a sensory mechanism—exaggerated sensory cortical representation of threat—in the pathogenic model of anxiety.[64]

## STAR★METHODS

Detailed methods are provided in the online version of this paper and include the following:

- KEY RESOURCES TABLE
- RESOURCE AVAILABILITY

## SUPPLEMENTAL INFORMATION

Supplemental information can be found online at https://doi.org/10.1016/j.cub.2022.02.076.

## ACKNOWLEDGMENTS

This research was supported by the National Institute of Mental Health (R01MH093413 and R21MH126479 to W.L.) and the FSU Chemical Senses Training (CTP) grant (T32DC000044 to K.J.C.) from the National Institutes of Health (NIH/NIDCD). We thank Joshua Brown and Chris Martin for helpful comments.

## AUTHOR CONTRIBUTIONS

Y.Y. and W.L. designed the experiment; Y.Y., L.R.N., and K.J.C. collected data; Y.Y., L.R.N., K.J.C., and W.L. performed analysis; Y.Y., L.R.N., K.J.C., and W.L. wrote the manuscript.

## DECLARATION OF INTERESTS

The authors declare no competing interests.

Received: November 13, 2021
Revised: January 18, 2022
Accepted: February 28, 2022
Published: March 23, 2022

## REFERENCES

1. LeDoux, J.E. (2000). Emotion circuits in the brain. Annu. Rev. Neurosci. *23*, 155–184.
2. Pessoa, L., and Adolphs, R. (2010). Emotion processing and the amygdala: from a "low road" to "many roads" of evaluating biological significance. Nat. Rev. Neurosci. *11*, 773–783.
3. LeDoux, J. (2012). Rethinking the emotional brain. Neuron *73*, 653–676. https://doi.org/10.1016/j.neuron.2012.02.004.
4. Ressler, K.J. (2020). Translating across circuits and genetics toward progress in fear-and anxiety-related disorders. Am. J. Psychiatry *177*, 214–222.
5. Grosso, A., Cambiaghi, M., Concina, G., Sacco, T., and Sacchetti, B. (2015). Auditory cortex involvement in emotional learning and memory. Neuroscience *299*, 45–55.
6. Weinberger, N.M., and Bieszczad, K.M. (2011). Introduction: from traditional fixed cortical Sensationism to contemporary plasticity of primary sensory cortical representations. In Neurobiology of Sensation and Reward, J.A. Gottfried, ed. (CRC Press), pp. 3–13.
7. Li, W. (2014). Learning to smell danger: acquired associative representation of threat in the olfactory cortex. Front. Behav. Neurosci. *8*, 98.
8. Wilson, D.A., and Sullivan, R.M. (2011). Cortical processing of odor objects. Neuron *72*, 506–519.
9. McGann, J.P. (2015). Associative learning and sensory neuroplasticity: how does it happen and what is it good for? Learn. Mem. *22*, 567–576.
10. Wilson, D.A. (2009). Pattern separation and completion in olfaction. Ann. N. Y. Acad. Sci. *1170*, 306–312.
11. Hunsaker, M.R., and Kesner, R.P. (2013). The operation of pattern separation and pattern completion processes associated with different attributes or domains of memory. Neurosci. Biobehav. Rev. *37*, 36–58. https://doi.org/10.1016/j.neubiorev.2012.09.014.
12. Weinberger, N.M. (2007). Associative representational plasticity in the auditory cortex: a synthesis of two disciplines. Learn. Mem. *14*, 1–16.
13. Suga, N. (2012). Tuning shifts of the auditory system by corticocortical and corticofugal projections and conditioning. Neurosci. Biobehav. Rev. *36*, 969–988. https://doi.org/10.1016/j.neubiorev.2011.11.006.
14. You, Y., Brown, J., and Li, W. (2021). Human sensory cortex contributes to the long-term storage of aversive conditioning. J. Neurosci. *41*, 3222–3233. https://doi.org/10.1523/JNEUROSCI.2325-20.2021.
15. Ojala, K.E., Staib, M., Gerster, S., Ruff, C.C., and Bach, D.R. (2022). Inhibiting human aversive memory by transcranial theta-burst stimulation to primary sensory cortex. Biol. Psychiatry. Published online February *10*, 2022. https://doi.org/10.1016/j.biopsych.2022.01.021.
16. Barnes, D.C., Hofacer, R.D., Zaman, A.R., Rennaker, R.L., and Wilson, D.A. (2008). Olfactory perceptual stability and discrimination. Nat. Neurosci. *11*, 1378–1380. https://doi.org/10.1038/nn.2217.
17. Chapuis, J., and Wilson, D.A. (2011). Bidirectional plasticity of cortical pattern recognition and behavioral sensory acuity. Nat. Neurosci. *15*, 155–161.
18. McTeague, L.M., Gruss, L.F., and Keil, A. (2015). Aversive learning shapes neuronal orientation tuning in human visual cortex. Nat. Commun. *6*, 7823. https://doi.org/10.1038/ncomms8823.
19. Weinberger, N.M. (2007). Auditory associative memory and representational plasticity in the primary auditory cortex. Hear. Res. *229*, 54–68.
20. Weinberger, N.M. (2004). Specific long-term memory traces in primary auditory cortex. Nat. Rev. Neurosci. *5*, 279–290.
21. Suga, N., and Ma, X. (2003). Multiparametric corticofugal modulation and plasticity in the auditory system. Nat. Rev. Neurosci. *4*, 783–794.
22. Cambiaghi, M., Grosso, A., Likhtik, E., Mazziotti, R., Concina, G., Renna, A., Sacco, T., Gordon, J.A., and Sacchetti, B. (2016). Higher-order sensory cortex drives basolateral amygdala activity during the recall of remote, but not recently learned fearful memories. J. Neurosci. *36*, 1647–1659.
23. Yang, Y., Liu, D.Q., Huang, W., Deng, J., Sun, Y., Zuo, Y., and Poo, M.M. (2016). Selective synaptic remodeling of amygdalocortical connections associated with fear memory. Nat. Neurosci. *19*, 1348–1355.
24. Dalmay, T., Abs, E., Poorthuis, R.B., Hartung, J., Pu, D.L., Onasch, S., Lozano, Y.R., Signoret-Genest, J., Tovote, P., Gjorgjieva, J., et al. (2019). A critical role for neocortical processing of threat memory. Neuron *104*, 1180–1194.e7. https://doi.org/10.1016/j.neuron.2019.09.025.
25. Sacco, T., and Sacchetti, B. (2010). Role of secondary sensory cortices in emotional memory storage and retrieval in rats. Science *329*, 649–656.
26. Kwon, J.T., Jhang, J., Kim, H.S., Lee, S., and Han, J.H. (2012). Brain region-specific activity patterns after recent or remote memory retrieval of auditory conditioned fear. Learn. Mem. *19*, 487–494.
27. Grosso, A., Cambiaghi, M., Renna, A., Milano, L., Merlo, G.R., Sacco, T., and Sacchetti, B. (2015). The higher order auditory cortex is involved in the assignment of affective value to sensory stimuli. Nat. Commun. *6*, 1–14.
28. Grosso, A., Cambiaghi, M., Milano, L., Renna, A., Sacco, T., and Sacchetti, B. (2017). Region-and layer-specific activation of the higher order auditory

cortex Te2 after remote retrieval of fear or appetitive memories. Cereb. Cortex *27*, 3140–3151.

29. Li, W., Howard, J.D., Parrish, T.B., and Gottfried, J.A. (2008). Aversive learning enhances perceptual and cortical discrimination of indiscriminable odor cues. Science *319*, 1842–1845. https://doi.org/10.1126/science.1152837.
30. Padmala, S., and Pessoa, L. (2008). Affective learning enhances visual detection and responses in primary visual cortex. J. Neurosci. *28*, 6202–6210. https://doi.org/10.1523/JNEUROSCI.1233-08.2008.
31. Miskovic, V., and Keil, A. (2012). Acquired fears reflected in cortical sensory processing: a review of electrophysiological studies of human classical conditioning. Psychophysiology *49*, 1230–1241.
32. Shalev, L., Paz, R., and Avidan, G. (2018). Visual aversive learning compromises sensory discrimination. J. Neurosci. *38*, 2766–2779. https://doi.org/10.1523/JNEUROSCI.0889-17.2017.
33. Staib, M., and Bach, D.R. (2018). Stimulus-invariant auditory cortex threat encoding during fear conditioning with simple and complex sounds. NeuroImage *166*, 276–284.
34. Staib, M., Abivardi, A., and Bach, D.R. (2020). Primary auditory cortex representation of fear-conditioned musical sounds. Hum. Brain Mapp. *41*, 882–891.
35. Haberly, L.B. (2001). Parallel-distributed processing in olfactory cortex: new insights from morphological and physiological analysis of neuronal circuitry. Chem. Senses *26*, 551–576.
36. Gluck, M.A., and Granger, R. (1993). Computational models of the neural bases of learning and memory. Annu. Rev. Neurosci. *16*, 667–706. https://doi.org/10.1146/annurev.ne.16.030193.003315.
37. Weinberger, N.M. (1998). Physiological memory in primary auditory cortex: characteristics and mechanisms. Neurobiol. Learn. Mem. *70*, 226–251. https://doi.org/10.1006/nlme.1998.3850.
38. Serences, J.T., Ester, E.F., Vogel, E.K., and Awh, E. (2009). Stimulus-specific delay activity in human primary visual cortex. Psychol. Sci. *20*, 207–214. https://doi.org/10.1111/j.1467-9280.2009.02276.x.
39. Dubois, J., de Berker, A.O., and Tsao, D.Y. (2015). Single-unit recordings in the macaque face patch system reveal limitations of fMRI MVPA. J. Neurosci. *35*, 2791–2802. https://doi.org/10.1523/JNEUROSCI.4037-14.2015.
40. Davis, M. (1992). The role of the amygdala in fear and anxiety. Annu. Rev. Neurosci. *15*, 353–375.
41. Bienvenu, T.C.M., Dejean, C., Jercog, D., Aouizerate, B., Lemoine, M., and Herry, C. (2021). The advent of fear conditioning as an animal model of post-traumatic stress disorder: learning from the past to shape the future of PTSD research. Neuron *109*, 2380–2397. https://doi.org/10.1016/j.neuron.2021.05.017.
42. Bakin, J.S., and Weinberger, N.M. (1990). Classical conditioning induces CS-specific receptive field plasticity in the auditory cortex of the guinea pig. Brain Res. *536*, 271–286. https://doi.org/10.1016/0006-8993(90)90035-a.
43. Aizenberg, M., and Geffen, M.N. (2013). Bidirectional effects of aversive learning on perceptual acuity are mediated by the sensory cortex. Nat. Neurosci. *16*, 994–996.
44. Chen, C.F., Barnes, D.C., and Wilson, D.A. (2011). Generalized vs. stimulus-specific learned fear differentially modifies stimulus encoding in primary sensory cortex of awake rats. J. Neurophysiol. *106*, 3136–3144.
45. Pavlov, I.P. (1927). Conditioned Reflexes, transl., G.V. Anrep, ed. (Oxford)
46. Lissek, S., Biggs, A.L., Rabin, S.J., Cornwell, B.R., Alvarez, R.P., Pine, D.S., and Grillon, C. (2008). Generalization of conditioned fear-potentiated startle in humans: experimental validation and clinical relevance. Behav. Res. Ther. *46*, 678–687. https://doi.org/10.1016/j.brat.2008.02.005.
47. Dunsmoor, J.E., and Paz, R. (2015). Fear generalization and anxiety: behavioral and neural mechanisms. Biol. Psychiatry *78*, 336–343.
48. Kent, B.A., Hvoslef-Eide, M., Saksida, L.M., and Bussey, T.J. (2016). The representational-hierarchical view of pattern separation: not just hippocampus, not just space, not just memory? Neurobiol. Learn. Mem. *129*, 99–106.
49. Yassa, M.A., and Stark, C.E.L. (2011). Pattern separation in the hippocampus. Trends Neurosci. *34*, 515–525. https://doi.org/10.1016/j.tins.2011.06.006.
50. Quian Quiroga, R. (2020). No pattern separation in the human hippocampus. Trends Cogn. Sci. *24*, 994–1007. https://doi.org/10.1016/j.tics.2020.09.012.
51. Li, W., Luxenberg, E., Parrish, T., and Gottfried, J.A. (2006). Learning to smell the roses: experience-dependent neural plasticity in human piriform and orbitofrontal cortices. Neuron *52*, 1097–1108. https://doi.org/10.1016/j.neuron.2006.10.026.
52. Gottfried, J.A. (2010). Central mechanisms of odour object perception. Nat. Rev. Neurosci. *11*, 628–641. https://doi.org/10.1038/nrn2883.
53. Roesch, M.R., Stalnaker, T.A., and Schoenbaum, G. (2007). Associative encoding in anterior piriform cortex versus orbitofrontal cortex during odor discrimination and reversal learning. Cereb. Cortex *17*, 643–652. https://doi.org/10.1093/cercor/bhk009.
54. Howard, J.D., and Kahnt, T. (2017). Identity-specific reward representations in orbitofrontal cortex are modulated by selective devaluation. J. Neurosci. *37*, 2627–2638. https://doi.org/10.1523/JNEUROSCI.3473-16.2017.
55. Howard, J.D., Kahnt, T., and Gottfried, J.A. (2016). Converging prefrontal pathways support associative and perceptual features of conditioned stimuli. Nat. Commun. *7*, 11546. https://doi.org/10.1038/ncomms11546.
56. Brewin, C.R., Gregory, J.D., Lipton, M., and Burgess, N. (2010). Intrusive images in psychological disorders: characteristics, neural mechanisms, and treatment implications. Psychol. Rev. *117*, 210–232. https://doi.org/10.1037/a0018113.
57. Brewin, C.R. (2014). Episodic memory, perceptual memory, and their interaction: foundations for a theory of posttraumatic stress disorder. Psychol. Bull. *140*, 69–97. https://doi.org/10.1037/a0033722.
58. Michael, T., Ehlers, A., Halligan, S.L., and Clark, D.M. (2005). Unwanted memories of assault: what intrusion characteristics are associated with PTSD? Behav. Res. Ther. *43*, 613–628. https://doi.org/10.1016/j.brat.2004.04.006.
59. Ehlers, A., Hackmann, A., Steil, R., Clohessy, S., Wenninger, K., and Winter, H. (2002). The nature of intrusive memories after trauma: the warning signal hypothesis. Behav. Res. Ther. *40*, 995–1002. https://doi.org/10.1016/s0005-7967(01)00077-8.
60. Clancy, K.J., Albizu, A., Schmidt, N.B., and Li, W. (2020). Intrinsic sensory disinhibition contributes to intrusive re-experiencing in combat veterans. Sci. Rep. *10*, 936.
61. Krusemark, E.A., and Li, W. (2011). Do all threats work the same way? Divergent effects of fear and disgust on sensory perception and attention. J. Neurosci. *31*, 3429–3434. https://doi.org/10.1523/JNEUROSCI.4394-10.2011.
62. Krusemark, E.A., and Li, W. (2013). From early sensory specialization to later perceptual generalization: dynamic temporal progression in perceiving individual threats. J. Neurosci. *33*, 587–594. https://doi.org/10.1523/JNEUROSCI.1379-12.2013.
63. You, Y., and Li, W. (2016). Parallel processing of general and specific threat during early stages of perception. Soc. Cogn. Affect. Neurosci. *11*, 395–404. https://doi.org/10.1093/scan/nsv123.
64. Li, W. (2019). Perceptual mechanisms of anxiety and its disorders. In Cambridge Handbook of Anxiety and Related Disorders, B. Olatunji, ed. (Cambridge Press).
65. Carver, C.S., and White, T.L. (1994). Behavioral inhibition, behavioral activation, and affective responses to impending reward and punishment: the BIS/BAS scales. J. Pers. Soc. Psychol. *67*, 319–333.
66. Zinbarg, R.E., and Mohlman, J. (1998). Individual differences in the acquisition of affectively valenced associations. J. Pers. Soc. Psychol. *74*, 1024–1040.

67. Gray, J.A., and McNaughton, N. (2000). The Neuropsychology of Anxiety:an Enquiry into the Functions of the Septo-Hippocampal System, Second Edition (Oxford University Press).
68. Krusemark, E.A., Novak, L.R., Gitelman, D.R., and Li, W. (2013). When the sense of smell meets emotion: anxiety-state-dependent olfactory processing and neural circuitry adaptation. J. Neurosci. *33*, 15324–15332.
69. Novak, L.R., Gitelman, D.R., Schuyler, B., and Li, W. (2015). Olfactory-visual integration facilitates perception of subthreshold negative emotion. Neuropsychologia *77*, 288–297. https://doi.org/10.1016/j.neuropsychologia.2015.09.005.
70. Lang, P., Bradley, M., and Cuthbert, B. (2008). International Affective Picture System (IAPS): Affective Ratings of Pictures and Instruction Manual. Technical Report A-8 (Gainesville: University of Florida).
71. Hawk, S.T., Van Kleef, G.A., Fischer, A.H., and Van Der Schalk, J. (2009). "Worth a thousand words": absolute and relative decoding of nonlinguistic affect vocalizations. Emotion *9*, 293–305.
72. Forscher, E.C., and Li, W. (2012). Hemispheric asymmetry and visuo-olfactory integration in perceiving subthreshold (micro) fearful expressions. J. Neurosci. *32*, 2159–2165.
73. Lorig, T.S., Elmes, D.G., Zald, D.H., and Pardo, J.V. (1999). A computer-controlled olfactometer for fMRI and electrophysiological studies of olfaction. Behav. Res. Methods Instrum. Comput. *31*, 370–375. https://doi.org/10.3758/bf03207734.
74. Onat, S., and Büchel, C. (2015). The neuronal basis of fear generalization in humans. Nat. Neurosci. *18*, 1811–1818.
75. Abdulrahman, H., and Henson, R.N. (2016). Effect of trial-to-trial variability on optimal event-related fMRI design: implications for Beta-series correlation and multi-voxel pattern analysis. Neuroimage *125*, 756–766. https://doi.org/10.1016/j.neuroimage.2015.11.009.
76. Rorden, C., and Brett, M. (2000). Stereotaxic display of brain lesions. Behav. Neurol. *12*, 191–200. https://doi.org/10.1155/2000/421719.
77. Gottfried, J.A., and Zald, D.H. (2005). On the scent of human olfactory orbitofrontal cortex: meta-analysis and comparison to non-human primates. Brain Res. Brain Res. Rev. *50*, 287–304. https://doi.org/10.1016/j.brainresrev.2005.08.004.
78. Howard, J.D., Plailly, J., Grueschow, M., Haynes, J.D., and Gottfried, J.A. (2009). Odor quality coding and categorization in human posterior piriform cortex. Nat. Neurosci. *12*, 932–938. https://doi.org/10.1038/nn.2324.
79. Mai, J.K., Majtanik, M., and Paxinos, G. (2015). Atlas of the Human Brain (Academic Press).
80. Kriegeskorte, N., Mur, M., and Bandettini, P. (2008). Representational similarity analysis - connecting the branches of systems neuroscience. Front. Syst. Neurosci. *2*, 4. https://doi.org/10.3389/neuro.06.004.2008.
81. Poldrack, R.A., and Farah, M.J. (2015). Progress and challenges in probing the human brain. Nature *526*, 371–379. https://doi.org/10.1038/nature15692.
82. Bracci, S., Caramazza, A., and Peelen, M.V. (2015). Representational similarity of body parts in human occipitotemporal cortex. J. Neurosci. *35*, 12977–12985. https://doi.org/10.1523/JNEUROSCI.4698-14.2015.

## STAR★METHODS

### KEY RESOURCES TABLE

| REAGENT or RESOURCE | SOURCE | IDENTIFIER |
|---|---|---|
| Deposited data | | |
| Experiment stimuli | This study | https://github.com/LiLabFSU/Threat-memory-in-human-olfactory-cortex |
| Data (fMRI &behavioral) | This study | https://github.com/LiLabFSU/Threat-memory-in-human-olfactory-cortex |
| Analysis scripts | This study | https://github.com/LiLabFSU/Threat-memory-in-human-olfactory-cortex |
| Software and algorithms | | |
| MATLAB, v2021a | Mathworks | RRID: SCR_001622 |
| SPSS statistics, v28 | IBM | RRID: SCR_019096 |
| SPM, v12 | Wellcome Centre for Human Neuroimaging | RRID: SCR_007037 |
| Cogent 2000, v25 | Wellcome Centre for Human Neuroimaging | RRID: SCR_015672 |
| AcqKnowledge | Biopac Systems | RRID: SCR_014279 |

### RESOURCE AVAILABILITY

#### Lead contact

Further information and requests for resources should be directed to and will be fulfilled by the lead contact, Wen Li (wenli@psy.fsu.edu).

#### Materials availability

All experiment stimuli are publicly available at a repository (https://github.com/LiLabFSU/Threat-memory-in-human-olfactory-cortex). This study did not generate new unique reagents.

#### Data and code availability

- Anonymized data, including fMRI, behavioral, SCR and respiratory data, have been deposited at a repository (https://github.com/LiLabFSU/Threat-memory-in-human-olfactory-cortex), as listed in the key resources table. They are publicly available as of the date of publication.
- Analysis scripts have been deposited at a repository (https://github.com/LiLabFSU/Threat-memory-in-human-olfactory-cortex), as listed in the key resources table. They are publicly available as of the date of publication.
- Any additional information required to reanalyze the data reported in this paper is available from the lead contact upon request.

### EXPERIMENTAL MODEL AND SUBJECT DETAILS

#### Participants

Thirty-three individuals (13 males; age 19.9 ± 2.0 years, range 18–25) participated in this two-session fMRI experiment in exchange for course credit or monetary compensation. All participants were right-handed, with normal olfaction and normal or corrected-to-normal vision. Participants were screened to exclude acute nasal infections or allergies affecting olfaction, any history of severe head injury, psychological/neurological disorders, or current use of psychotropic medication. All participants provided informed consent to participate in the study, which was approved by the University of Wisconsin-Madison Institutional Review Board. One participant who failed to provide risk ratings on Day 1 and another who failed to follow the ODT task instruction were excluded from the corresponding analyses. Two participants were excluded from fMRI analysis due to metal artefact and excessive movement.

### METHOD DETAILS

#### Anxiety assessment

We used the Behavioral Inhibition Scale (BIS) to measure trait anxiety.[65] The BIS is a 7-item self-report questionnaire (score range: 7-28) measuring the strength of the behavioral inhibition system and threat sensitivity, known to reflect trait anxiety. This scale is

neurobiologically motivated, with high reliability and strong predictive validity of anxiety,[66,67] and recommended by the National Institute of Mental Health (NIMH) to measure the construct of "potential threat (anxiety)".

### Stimuli

We included two neutral odorants, acetophenone (5% l/l; diluted in mineral oil) and eugenol (18% l/l). These odors have received similar ratings on valence, intensity, familiarity, and pungency and been used as neutral odors in previous research.[68,69] They were labeled as odors "A" and "B" to the participants and were parametrically mixed into five mixtures to create a linear morphing continuum: 80% A/20% B, 65% A/35% B, 50% A/50% B, 35% A/65% B, and 20% A/80% B (Figure 1A). The two extreme mixtures (20% A/80% B and 80% A/20% B) served as conditioned stimuli (CS), differentially conditioned as threat CS (CSt) and safety CS (CSs), counterbalanced across participants, via pairings with threat and neutral unconditioned stimuli (UCS), respectively. The three intermediate mixtures were non-conditioned stimuli (nCS) and denoted as nCSt (neighboring odor of the CSt), nCSm (midpoint of the continuum), and nCSs (neighboring odor of the CSs), respectively. The UCS were bimodal (visuo-auditory) stimuli, including 7 pairs of disgust images (three depicting dirty toilets and four vomits) and disgust sounds (i.e., vomiting) and 7 pairs of neutral images (household objects) and neutral sounds. Images were chosen from the International Affective Picture Set (IAPS)[70] and internet sources.[63] Disgust sounds were from the disgust subset of human affective vocalizations,[71] and neutral sounds were pure tones (300, 500, and 800 Hz). Skin conductance response (SCR) data confirmed effectiveness of the aversive (vs. neutral) UCS (Figure 1A).

Odor stimuli were delivered at room temperature using an MRI-compatible sixteen-channel computer-controlled olfactometer (airflow set at 1.5 L/min), which permits rapid odor delivery in the absence of tactile, thermal or auditory confounds.[68,72,73] Stimulus presentation and collection of responses were controlled using Cogent2000 software (Wellcome Department of Imaging Neuroscience, London, UK) as implemented in Matlab (Mathworks, Natick, MA).

### Unconditioned skin conductance response (SCR)

SCR was acquired with BioPac MP150 (BIOPAC systems, Goleta, CA) from two MRI-compatible Ag/AgCl electrodes placed on the middle phalanx of the second and third digits of the non-dominant (left) hand at a sampling rate of 1000 Hz. A low-pass filter (0.5 Hz) was applied offline to eliminate MRI scanning artifacts. For each trial, evoked SCR response was defined by the magnitude of trough-to-peak SCR deflection during the interval between 0.5 s pre- and 7 s post-UCS onset (ITI = 14.1 s), with a minimal evoked deflection of 0.02 μS. We compared SCR evoked by the aversive and neutral UCS during conditioning. In support of its effectiveness, the aversive UCS produced significantly greater SCR than did the neutral UCS ($t$= 2.88, $p$ =.007; Figures 1A and S1).

### Odor discrimination task (ODT)

During the two-alternative forced-choice odor discrimination task (2-AFC ODT), each trial began with a visual "Get Ready" cue, followed by a 3-2-1 countdown and a sniffing cue, upon which participants were to take a steady and consistent sniff and respond whether the odor smelled like Odor A or B by button pressing (Figure 1B). Each of the five odor mixtures was presented 15 times, in a pseudo-random order without repetition over two consecutive trials. Seven additional trials with a central, blank rectangle on the screen (no response required) were randomly intermixed with the odor trials to help minimize olfactory fatigue and establish a non-odor fMRI baseline. Trials recurred with a stimulus onset asynchrony of 14.1 s.

### Experiment procedure

#### *Pre-experiment screening*

Approximately a week before the experiment, participants visited the lab to be screened for normal olfactory perception. They were also introduced to acetophenone and eugenol as Odors "A" and "B" and practiced on a 2-AFC ODT between the two odors. They also provided ratings on the five odor mixtures. We performed analyses on odor ratings to exclude confounds related to inherent odor stimulus differences. Baseline ratings for all five odor mixtures on valence, intensity, familiarity, and pungency were submitted to separate repeated-measures ANOVAs, which revealed no significant difference among five odor mixtures on any of the scales (all $F$ values < 1.61, all $P$ values > 0.182).

#### *Experiment day 1*

Participants first performed the 2-AFC ODT, then underwent differential conditioning, and then repeated the 2-AFC ODT (Figure 1C). During differential conditioning, CSt and CSs odors were presented (seven trials each, randomly intermixed; ITI = 12 s) for 1.8 s while the aversive or neutral UCS were presented respectively for 1.5 s at 1 s after CS odor onset, with 100% contingency. To prevent extinction by the repeated unreinforced CS presentation during the postconditioning 2-AFC ODT (on both Day 1 and Day 9), five extra trials of CSt paired with the aversive UCS were randomly inserted.[14,29,30,74] Data from these trials were excluded from analysis. After the postconditioning ODT, the five odor mixtures were presented (three trials per odor mixture, randomly intermixed), to which participants performed risk rating (likelihood of an aversive UCS to follow the odor) on a VAS of 0–100%.

#### *Experiment day 9*

Participants repeated the 2-AFC ODT and risk rating. After that, participants underwent an independent olfactory localizer scan involving a simple odor detection task, from which functional ROIs were extracted. Four additional odorants (α-ionone, citronellol, methyl cedryl ketone, 2-methoxy-4-methylphenol), neutral in valence and matched for intensity, were presented in this task (15 trials/odor), pseudo-randomly intermixed with 30 air-only trials.

### Respiratory monitoring

Respiration measurements were acquired (1000 Hz) during the ODT, using a BioPac MP150 (AcqKnowledge software) with a breathing belt affixed to the participant's chest to record abdominal or thoracic contraction and expansion. For each odor trial, a sniff waveform was extracted from a 6 s window post sniff onset and was baseline-corrected by subtracting the mean activity within 1 s preceding sniff onset. Sniff parameters (inspiratory volume, peak amplitude, and peak latency) were generated by averaging across all 15 trials per odor. We examined respiration parameters during the 2-AFC ODT, including peak amplitude, peak latency, and sniff inspiratory volume. ANOVAs (Odor X Time) on these sniff parameters revealed no effects of odor or odor-by-time interactions (all $P$ values > 0.095). These results thus ruled out variations in sniffing as potential confounds.

### Imaging acquisition and preprocessing

Gradient-echo T2 weighted echoplanar images (EPI) were acquired with blood-oxygen-level-dependent (BOLD) contrast and sagittal acquisition on a 3T GE MR750 MRI scanner. Imaging parameters were TR/TE = 2350/20 ms; flip angle = 60°, field of view = 220 mm, slice thickness = 2 mm, gap = 1 mm; in-plane resolution/voxel size = 1.72×1.72 mm; matrix size = 128×128. A field map was acquired with a gradient echo sequence, which was coregistered with EPI images to correct EPI distortions due to susceptibility. A high-resolution ($1\times1\times1mm^3$) T1-weighted anatomical scan was acquired. Five scan runs, including preconditioning, conditioning, Day 1 post-conditioning, Day 9 postconditioning, and odor localizer, were acquired. Six "dummy" scans from the beginning of each scan run were discarded to allow stabilization of longitudinal magnetization. Imaging data were preprocessed in SPM12 (www.fil.ion.ucl.ac.uk/spm), where EPI images were slice-time corrected, realigned, and field-map corrected. Images collected on both Day 1 and Day 9 sessions were spatially realigned to the first image of the first scan run on Day 1, while the high-resolution T1-weighted scan was co-registered to the averaged EPI of both scan sessions. All multivariate pattern analyses were conducted on EPI data that were neither normalized nor smoothed to preserve signal information at the level of individual voxels, scans, and participants.

A general linear model (GLM) was computed on preconditioning ODT, conditioning, Day 1 postconditioning ODT, and Day 9 post-conditioning ODT scans. Applying the Least Squares All (LSA) algorithm, we set each odor trial as a separate regressor, convolved with a canonical hemodynamic response function.[75] Six movement-related regressors (derived from spatial realignment) were included to regress out motion-related variance. For the odor localizer scan, we applied a GLM with odor and no odor conditions as regressors, convolved with a canonical hemodynamic response function and the temporal and dispersion derivatives, besides the six motion regressors of no interest. A high-pass filter (cut-off, 128 s) was applied to remove low-frequency drifts and an autoregressive model (AR1) was applied to account for temporal nonsphericity.

### ROI definition

All four ROIs (APC, PPC, $OFC_{olf}$, and amygdala) were manually drawn on each participant's T1 image in MRIcro[76] (Figure 1D). The olfactory OFC ($OFC_{olf}$) was defined by a meta-analysis[77] and a prior study,[78] and the other ROIs were defined by a human brain atlas.[79] Left and right hemisphere counterparts were merged into a single ROI. Functional constraints were applied to these anatomical ROIs based on the odor-no-odor contrast of the independent odor localizer scan for each participant, with a liberal threshold at $P< 0.5$ uncorrected.[29]

## QUANTIFICATION AND STATISTICAL ANALYSIS

### fMRI analysis

#### *Representational similarity analysis (RSA)*

The RSA uses correlations across multivoxel response patterns to indicate the degree of similarity in response patterns[80,81] and thus presents an effective test of pattern differentiation.[29] For each participant and every ODT session, trial-wise beta values were extracted for all voxels within a functionally constrained ROI, which were then averaged across all 15 trials for each odor mixture, resulting in an odor-specific linear vector of beta values across a given ROI. Pearson's correlation ($r$) was computed between all pairs of pattern vectors at each session, resulting in a 5 x 5 correlation matrix—the representational similarity matrix—for each session. To directly represent pattern differentiation, this matrix was converted into a representational dissimilarity matrix (RDM) by replacing the $r$ values with dissimilarity scores ($1 - r$).[82] To assess pattern differentiation, we computed a pattern differentiation index (PDI) based on the RDM matrix (dissimilarity/distance = 1- $r$), following Fisher's Z transformation: PDI = [(d1+ d4) – (d2 + d3)], reflecting the dissimilarity/distance of CSt and CSs from their neighboring nCS odors (nCSt and nCSs, d1 and d4 respectively), controlled by the dissimilarity/distance between the midpoint odor (nCSm) and its neighbors (d2 and d3).

#### *Tuning analysis*

We adopted a voxel-based tuning analysis used for visual sensory encoding[38,39] to assess olfactory cortical tuning. Trial-wise beta values (5 odors × 15 trials) for each voxel were normalized (by z-scoring) across trials after removing the trial-wise mean beta across the ROI, from which we calculated mutual information (MI) conveyed by each voxel about each odor (see below). As low MI values (i.e., minimal mutual dependence between the distribution of responses and odor) reflect indiscriminant or random responses to all odors, voxels with bottom 10% MI values in a given ROI were excluded.[38] Voxel-based tuning was defined by the odor mixture eliciting the largest beta (i.e., optimal odor). As such, each of the remaining voxels was classified into one of five odor classes. In line with animal tuning analysis,[12,42] we examined the voxels tuned to the neighboring odors (nCSs and nCSt) of the CS before conditioning

and measured their tuning shift to the CS (relative to the neighboring nCS odor/nCSm) after conditioning. Accordingly, we derived a tuning shift index (TSI) for Day 1 and Day 9 postconditioning: TSI = (% CSs – % nCSm) + (% CSt – % nCSm), reflecting the % of initially nCSs/nCSt voxels that became tuned to the neighboring CSs/CSt, respectively, relative to the % of initially nCSs/nCSt voxels that became tuned to the other neighboring odor—nCSm.

In terms of MI calculation, first, we converted the beta values into a discrete variable ($B$)by dividing the range of betas into a set of equidistant bins ($b$). The size of the bins was determined by Freedman-Diaconis' rule [bin size = (max($B$) – min($B$))/2*IQR*$n^{-1/3}$], where n is the number of trials ($n$ = 75). We selected the median bin size of all voxels within an ROI based on the preconditioning data and held it constant for the postconditioning sessions (Day 1 and Day 9). Next, we computed for each voxel the entropy of (discretized) responses ($B$) as follows:

$$H(B) = -\sum_{b\in B} p(b)log_2p(b)$$

where $p(b)$ is the proportion of trials whose responses fall into bin $b$. Then, we computed conditional entropy $H(B|o)$, the entropy of responses given knowledge of the odor condition, as follows:

$$H(B|o) = -\sum_{o\in O} p(o)\sum_{b\in B} p(b|o)log_2p(b|o)$$

where $p(b|o)$ is the proportion of trials falling into bin $b$ when responding to a certain odor ($o$). The index of $MI(B;O)$, i.e., the amount of information a voxel conveys for an odor, was calculated as the reduction in entropy of responses given knowledge of the odor condition:

$$MI(B;O) = H(B) - H(B|o)$$

## Statistical analysis

Using analyses of variance (ANOVAs) of Odor (five mixtures) and Time (day 1 postconditioning and day 9 postconditioning), we performed trend analysis over the odor continuum on risk ratings and ODT response to capture the warping of affective and perceptual spaces by conditioning. We hypothesized that affective learning via conditioning would change the baseline neutral trend to an ascending safety-to-threat trend (Figure 2A). We further hypothesized that differential conditioning would enhance perceptual discrimination of the CS, expanding odor quality distances between the CS and their neighboring odors; resulting changes in odor quality space (i.e., differential CS endorsement rates; postconditioning - preconditioning) would conform to a cubic trend, anchored by respective increase and decrease in "CSt" rate for the neighboring odors of CSt and CSs—nCSt and nCSs (Figure 2B). As for the neural mechanisms, i.e., enhanced pattern differentiation between the CS and similar (neighboring) nCS and tuning shift towards the CS, we conducted ANOVAs of ROI (APC/PPC) and Time (day 1 postconditioning and day 9 postconditioning) on differential PDI scores and TSI scores, respectively. Finally, we examined modulatory effects of anxiety using Pearson's correlation of BIS scores with behavioral and neural effects of conditioning. Significance threshold was set at $P < 0.05$. Given the clear *a priori* hypotheses, one-tailed tests were accepted and are explicitly noted in the Results (two-tailed tests are not explicitly noted). To protect for Type I error, only significant effects in the ANOVAs were followed up with hypothesis testing. Correlational analysis with anxiety involved multiple tests, which were corrected using the false discovery rate (FDR) criterion (i.e., FDR $P < 0.05$).